# Experimental Results of Foundation Rocking On a Natural Clay Deposit

**J.N. Phipps, J.C. Ashlock & S. Sritharan**
*Iowa State University, United States of America*

**SUMMARY:**
The earthquake engineering community has recently shown an increased interest in the seismic performance of rocking foundation systems. Many centrifuge experiments have been performed on rocking foundations thus far, but only a few field-scale verification tests have been attempted. The available centrifuge experiments have predominantly investigated small-scale model foundations on sandy soils. This paper describes a field-scale experimental study of a rocking foundation system on a natural clay soil deposit. The rocking foundation system consisted of a square concrete footing resting on the surface of the soil, with an attached structural assembly. The experimental program described herein involved subjecting the foundation-structure assembly to two test types; dynamic free vibration and quasi-static lateral cyclic loading, to produce rocking at large soil strains. Energy dissipation and stiffness degradation observed in the tests are discussed.

*Keywords: foundation, rocking, clay, interaction, cyclic*

## 1. INTRODUCTION

The earthquake engineering community has recently shown an increased interest in the performance of rocking foundation systems. Part of this increased interest stems from the potential for successfully dissipating seismic energy through rocking at the soil-structure interface and allowing the foundation to re-center following the earthquake. Attempts have been made to help design professionals theoretically model soil-structure interaction in terms of rocking behavior. Many centrifuge experiments have been performed on rocking foundations thus far, but only a few field-scale verification tests have been attempted. The available centrifuge experiments have predominantly focused on small-scale model foundations on sandy soils. The following describes a field-scale experiment of a rocking foundation system on a natural clay soil deposit, including the test results and data interpretaions.

## 2. EXPERIMENTAL PROCEDURE

### 2.1. Rocking System

The selected rocking foundation system consisted of a square concrete footing resting on the surface of the soil. The structural assembly, as shown in Fig. 2.1, consists of a concrete footing, steel threaded anchor rods, non-shrink levelling grout, a steel base plate, an AISC HP shape column, a massive rigid concrete pile cap, a servo-hydraulic inertial shaker, and steel plate counterweights. Refer to Table 2.1 for sizes and dimensions of the rocking system elements.

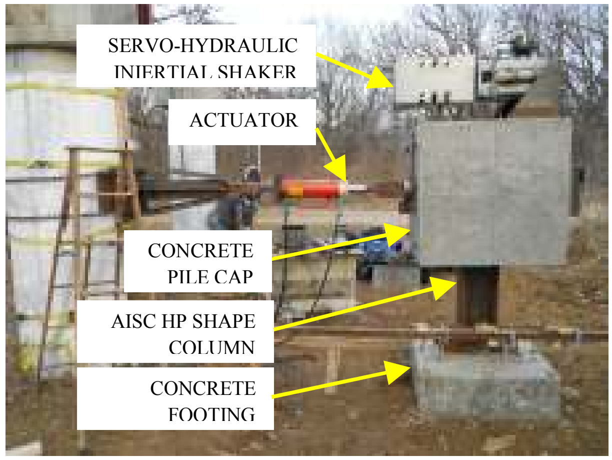


**Figure 2.1.** Structural assembly of rocking system

**Table 2.1.** Sizes and Dimensions of Rocking System Elements

| | |
|---|---|
| Concrete footing width (m) | 0.914 |
| Concrete footing height (m) | 0.308 |
| AISC HP column | HP10x42 |
| Column base plate thickness (m) | 0.0191 |
| Column base plate length (m) | 0.508 |
| Column base plate width (m) | 0.254 |
| Non-shrink grout thickness (mm) | ≈ 38.1 |
| Concrete pile cap width (m) | 0.914 |
| Concrete pile cap height (m) | 0.914 |

## 2.2. Experimental Program

The experimental program was designed so that the concrete cap attached to the pile head would be subjected to three types of horizontal loading to produce rocking: dynamic forced vibration using the shaker, dynamic free vibration using cable snap tests, and pseudo-static cyclic loading using an actuator. This paper will focus on the free vibration and pseudo-static test results. Both of these loading types produced large enough rotational displacements to induce uplift of the footing on both sides as the load reversals took place. The rocking foundation specimen was instrumented with string potentiometers and accelerometers to capture the response in the form of rotation and horizontal and vertical displacements. These signals were collected and processed with a custom-programmed National Instruments LabVIEW signal analyzer.

### *2.2.1. Free vibration snap tests*

The dynamic snap tests were performed by pulling the pile cap with a cable winch puller to create an initial rotation, then quickly releasing it to induce free vibration. A quick-release or snap mechanism was connected between the rocking system pile cap and a large reinforced concrete drilled shaft reaction column. Upon release of the snap mechanism, string potentiometers and accelerometers captured the free vibrations response of the rocking foundation.

### *2.2.2. Quasi-static lateral cyclic tests*

The quasi-static lateral cyclic tests were performed by applying horizontal displacements to the concrete pile cap from a doubly hinged hydraulic actuator mounted horizontally from a reaction frame, which was anchored to the large reinforced concrete reaction column. A load cell was used to measure the force applied at the connection of the actuator and pile cap. The pile cap was slowly pushed and pulled by the hydraulic jack in a quasi-static manner, so that the nonlinear hysteretic soil response could be isolated from the total dynamic response.

## 3. RESULTS

### 3.1. Free Vibration Snap Test Results

The accelerometers on the pile cap were used to compute the inertial force of the system in free vibration. Knowing the mass and centroid of the entire rocking system along with accelerations at discrete points, rigid body kinematics were used to calculate the centroidal acceleration and rotation. Five horizontal and three vertical string potentiometers (string pots) were installed on the concrete pile cap and concrete footing to measure displacements. The string pot signals were used to calculate the planar motion of the system. Similar to other rocking foundation studies of Gajan et al. (2004, 2005, 2008, 2009), the motion of the footing was characterized by the displacement of the bottom center point of the footing. Because displacements at the bottom center point of the footing were not directly measured, measurements from three string pots along with a simultaneous nonlinear system of equations were used to track the footing motion. Key assumptions for this formulation were that the footing behaved as a rigid body and no out of plane displacement or rotation occurred during the tests. The nonlinear formulation accounted for the large rotations of the string pot cables during rocking to triangulate the coordinates of the control point of the footing. The typical motion of a free vibration snap test is shown in Fig. 3.1.

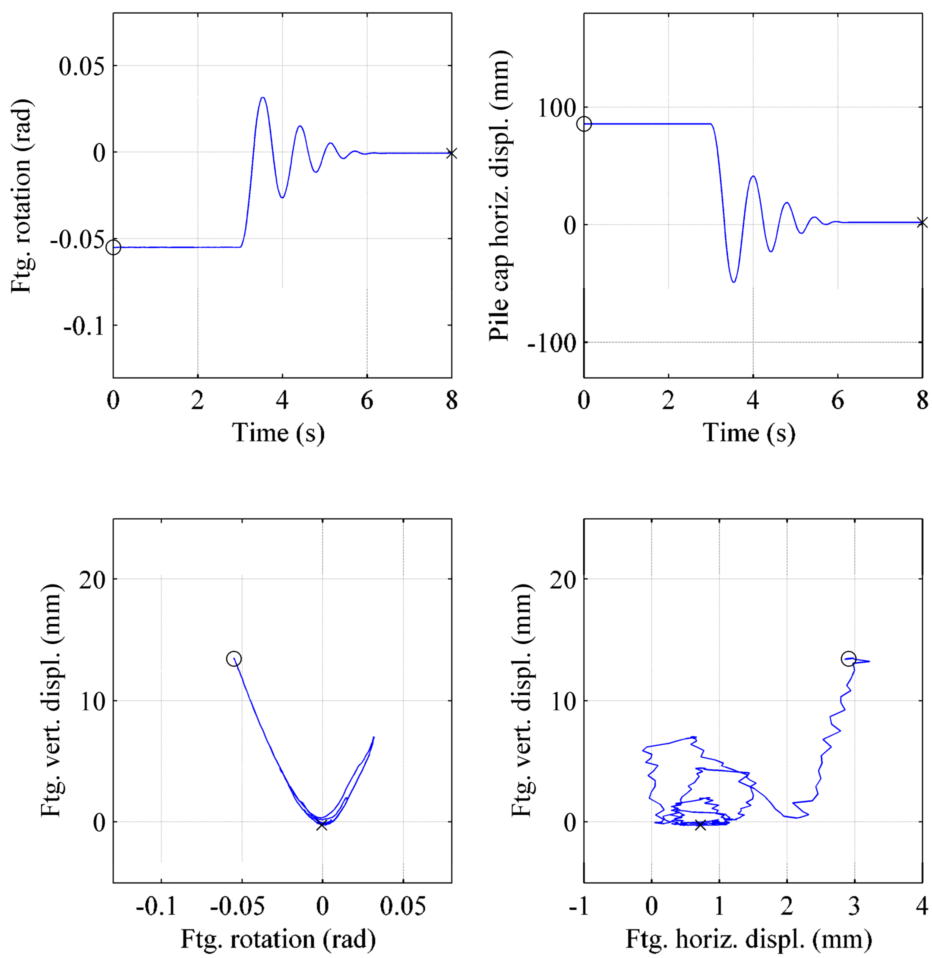


**Figure 3.1.** Rocking foundation response from a representative snap test (Snap04)

In general, as snap testing progressed from smaller to larger initial rotations, the damped period of the system increased as illustrated in Fig. 3.2. Increased period duration of rocking footings suggests that force demands imposed on a superstructure would be reduced (Bartlett 1976). Not only had the period changed from test to test under various initial rotations, but also from initial to subsequent cycles within a test, as illustrated in Fig. 3.3. In fact, the period of the second cycle of a test was shown to have decreased as much as 30-50% from the first cycle. Figure 3.2 shows the dramatic change in period from tests Snap01-Snap08 to Snap09-Snap11. Tests Snap01 through Snap08 were performed consecutively. Following test Snap08, quasi-static cyclic lateral tests were performed (Cyclic01 through Cyclic09), in which the soil was subjected to increasing strain and plastic deformation. Following the large-strain cyclic tests, the period of the first cycle of test Snap09 increased by approximately 20% relative to that of test Snap08.

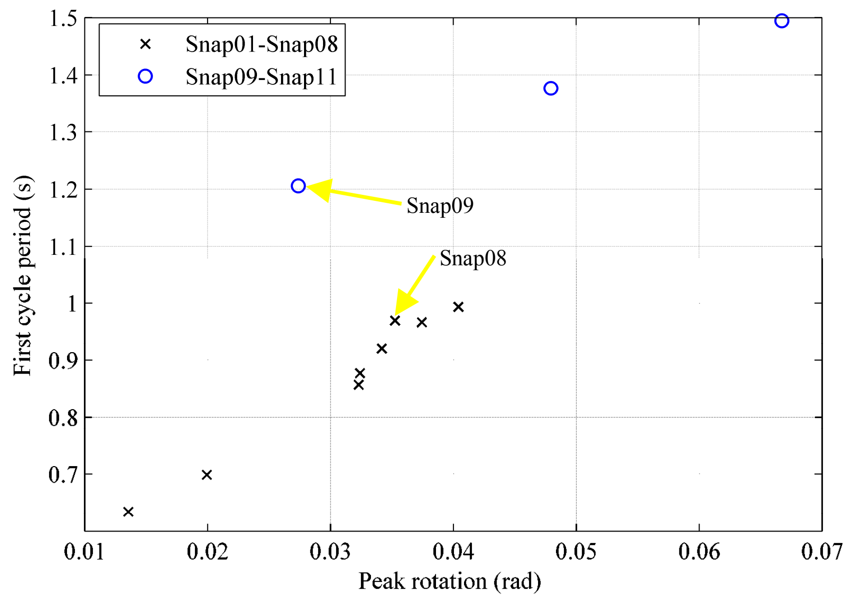


**Figure 3.2.** Period of the Rocking Foundation During First Cycle of Snap Tests

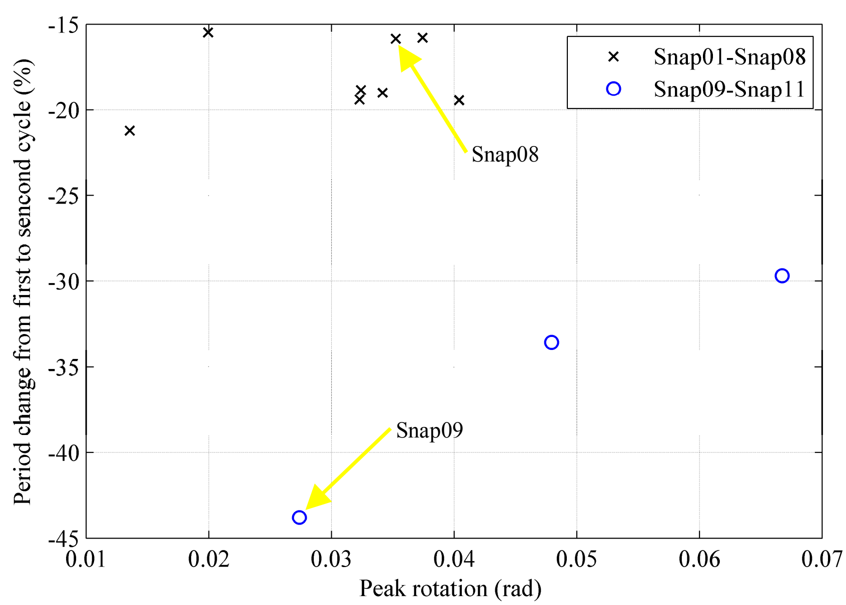


**Figure 3.3.** Period Change of the Rocking Foundation From First to Second Cycles of Snap Tests

The stiffness of the soil was believed to have been affected nonlinearly by localized yielding, and thus the natural frequency and period of the rocking system were also affected. Consequently, it is concluded that a rocking system on a foundation soil would not possess a fixed period since the soil stiffness changes throughout a test as well as between tests. Specifically, the backbone secant stiffness would be smaller at the beginning of a test and increases as the amplitude of oscillation decays during free vibration. Assigning a period to the system is further complicated by the rocking footing making impacts with soil at two rotation peaks. Since this is a field study on a heterogeneous natural soil deposit, each impact zone can uniquely affect the dynamic properties of the rocking system.

Figures 3.2 and 3.3 show the periodic changes of the rocking system in free vibration for snap tests. The change in the period of the system can be attributed to a reduced rotational stiffness at the soil-structure interface from soil yielding and nonlinear plastic rounding of the soil surface. The rounding of the soil surface is the basis for a recently developed rocking model known as the Contact Interface Model (CIM) developed by Gajan and Kutter (2009). The CIM is designed to model the nonlinear relationship between cyclic loads and displacements at the footing-soil interface. This model tracks the plastic deformations of a soil surface due to kinematics of the footing-soil system. Evaluation of the soil-structure rocking system in both free vibration and quasi-static lateral cyclic tests in this study indicates that the clayey soil indeed adopted a rounded surface. The rounding behavior is illustrated in the simple free body diagram of Fig. 3.4a, and was verified in the tests as shown in Fig. 3.4b and 3.4c. Figure 3.4a is a free body diagram from Gajan and Kutter (2010) depicting the footing length *L*, vertical load *V*, ultimate moment *Mult*, critical contact length *Lc*, resultant force *R*, bearing pressure *qult*, and resultant eccentricity *e_max*. Figures 3.4b and 3.4c illustrate that formation of the gaps and change in the length of contact between soil and footing as rounding of the soil surface develops.

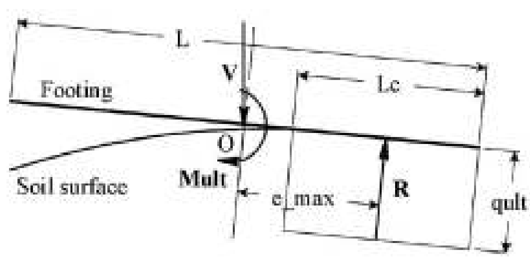


(a)

(b)

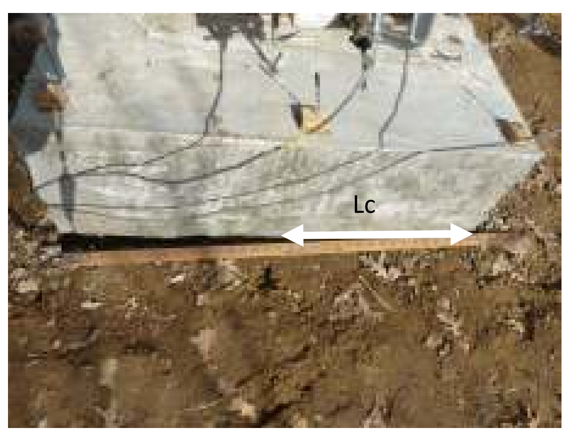


(c)

**Figure 3.4.** Example Quasi-Static Lateral Cyclic Test (Cyclic04). (a) definition of Contact Interface Model parameters (from Gajan and Kutter, 2009), (b) maximum measured uplift of 3.5 inches, (c) estimation of Lc measured by inserting feeler gage under footing.

### 3.2. Quasi-Static Lateral Cyclic Test Results

Figure 3.5 shows the moment-rotation, horizontal force-horizontal displacement, vertical displacement-rotation, and vertical displacement-horizontal displacement relationships at the base

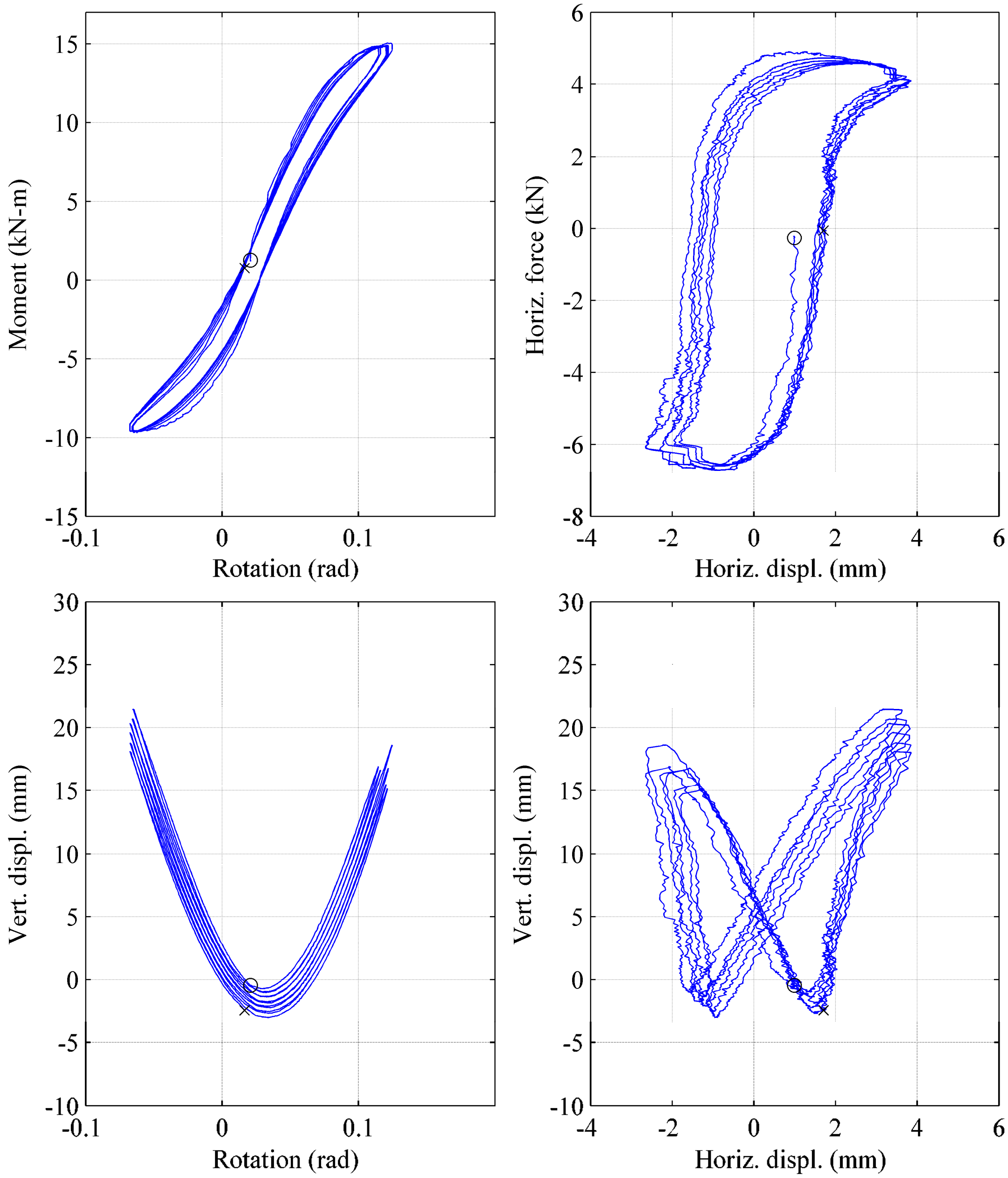


**Figure 3.5.** Response from Representative Quasi-Static Lateral Cyclic Test (Cyclic04**)**

center point of the rocking footing for the slow lateral cyclic tests. The moment-rotation and force-displacement plots quantify the amount of energy dissipated at the soil-footing interface. The results from the cyclic tests indicate that each test maintained moment capacity. Moment capacity was not observed to reduce significantly with respect to number of cycles or amplitude of rotation. As Fig. 3.6 indicates the rotational stiffness, however, decreased as the amplitude of rotation increased.

The vertical displacement-rotation plot of Fig. 3.5 illustrates the contact versus settlement behavior expected for rocking foundations on a clay soil. The rocking footing experienced uplift near peak rotations and a portion of the footing base lost contact with the soil. Yielding of the soil took place as the footing lost contact, as the portion remaining in contact maintained static equilibrium through an increase in contact pressure. As footing uplift and soil yielding continued, the cyclic lateral loading caused rounding of the soil surface, implying that gaps formed near both pivot points of the rocking footing. These gaps, in addition to the soil yielding under a changing contact area, contributed to the nonlinear moment-rotation relationship and the degradation of rotational stiffness. The troughs of the vertical displacement-rotation curves in Figure 3.5 also show the amount of permanent vertical deformation accumulated during a test. Each slow lateral cyclic test lasted between three and six cycles, resulting in small vertical settlements within each test. For example, approximately 2.5 mm of settlement is shown for the test of Fig. 3.5 having six cycles.

Similar to the maintaining of moment resistance, the horizontal force-horizontal displacement relationship clearly shows that horizontal force did not reduce with increasing number of cycles or amplitude of lateral displacement. Horizontal displacement was also observed to remain relatively unchanged until the peak shear capacity was reached, at which point the footing began to slide. In each full cyclic test, the area enclosed by the horizontal force-horizontal displacement loops indicates the amount of energy dissipated through each cycle in sliding and horizontal shearing strains.

The butterfly shapes of the vertical displacement-horizontal displacement plot show the coupling relationship between uplift and sliding. The base of the butterfly shape shows the two points at which the control point on the base of the footing landed, depending on which side was being uplifted. This phenomenon caused the footing to slide back and forth under cyclic lateral loading.

Elastic portions of the moment-rotation plots were used to evaluate the rotational stiffness degradation of the natural clay soil deposit in this study. These rotational stiffness values can be compared with Gazetas' (1991) elastic stiffness presented below for a rectangular footing:

$$k_{\theta,\max} = \frac{G_{MAX}}{1-\nu} I^{0.75} \left[ 3\left(\frac{L}{B}\right)^{0.15} \right] \beta \tag{3.1}$$

According to Seed and Idriss (1970), the initial shear modulus, *Gmax*, can be approximated by

$$G_{MAX} \simeq (1000 \text{ to } 2500) S_u \tag{3.2}$$

for a very stiff clay. Based on previous cone penetration tests at the Spangler test site reported by Shelman (2009), the undrained shear strength, $S_u$, was found to be approximately 1000 kPa at the "equivalent" depth of the zone of influence for a square footing on an inhomogeneous soil deposit. Gazetas (1991) reports that the "equivalent" depth of the zone of influence for the rocking mode of vibration can be approximated as

$$\frac{z}{B/2} = \frac{1}{3} \tag{3.3}$$

where $z$ is the "equivalent" soil depth and $B$ is the footing width. The Poisson's ratio of the soil, $\nu$, can be approximated as 0.25 for stiff clays (Gazetas 1991). The moment of inertia, $I$, can be computed about the centroid of the footing base normal to the direction of rocking. The footing length and width, $L$ and $B$, respectively, are equal for square footings. The embedment factor, $\beta$, is correlated with the ratio of the depth of embedment to the length of the footing (Gazetas 1991). For surface footings as tested in this study, $\beta$ was taken as unity.

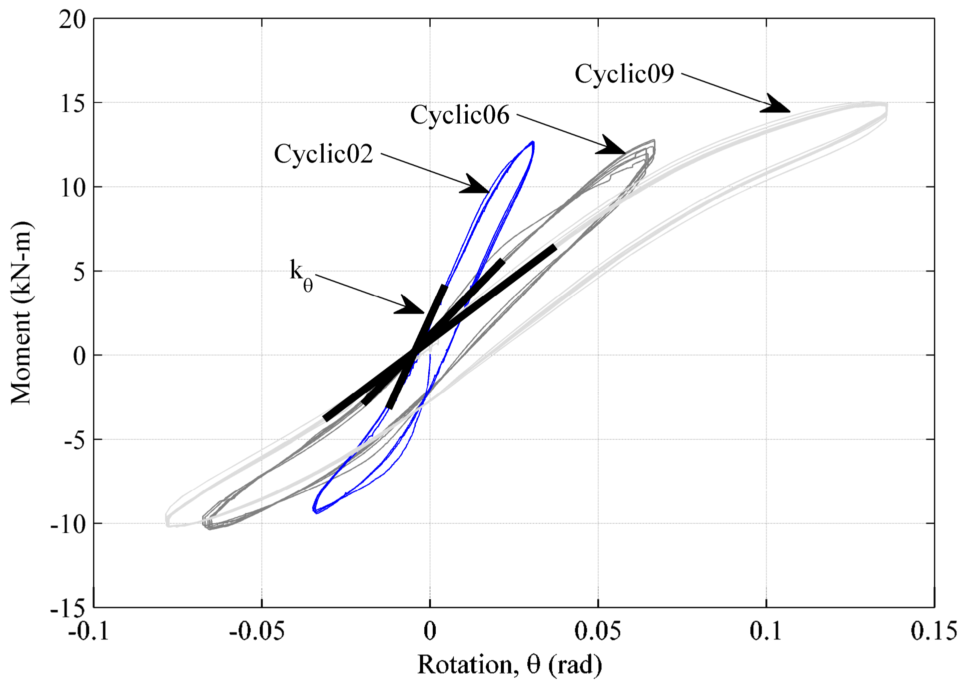


**Figure 3.6.** Moment-Rotation Plot Showing Rotational Stiffness Degradation for Slow Cyclic Tests

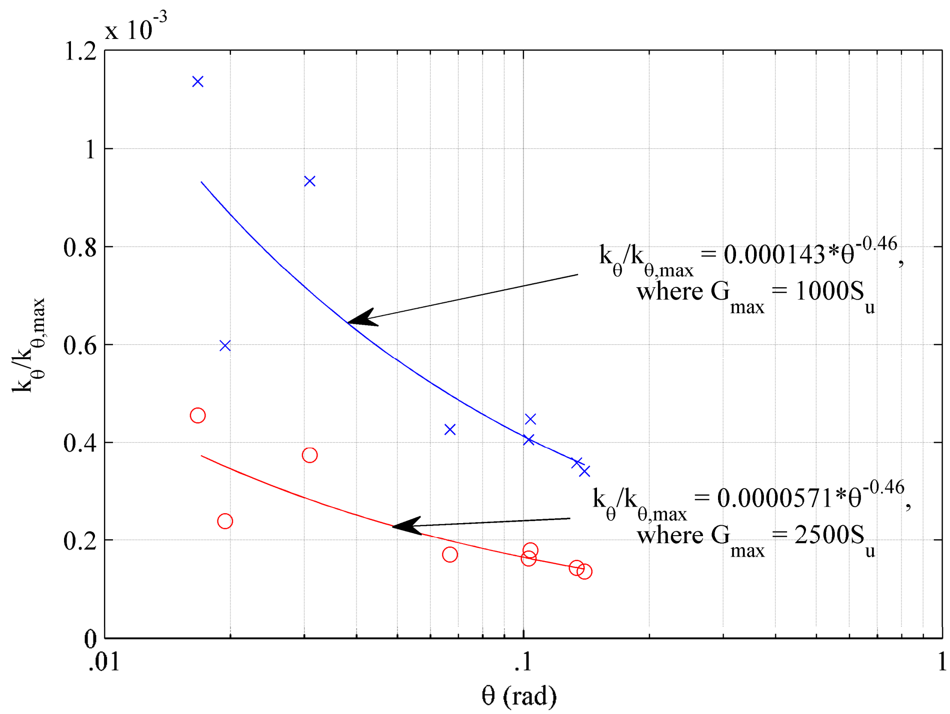


**Figure 3.7.** Rotational Stiffness Degradation versus Maximum Angle of Rotation for Slow Cyclic Tests

Figure 3.7 shows $k_\theta$ as determined from the slow cyclic tests normalized by $k_{\theta,max}$ given by Eqn. 3.1. The data from the cyclic tests were normalized against two levels of $k_{\theta,max}$, according to the upper and lower bounds of the estimated correlation of $G_{max}$ with regard to $S_u$ in Eqn. 3.2. A mean stiffness reduction trend was computed for each level of rotational stiffness, resulting in

$$\frac{k_\theta}{k_{\theta,\max}} = 1.43\times10^{-4}\left(\theta^{-0.46}\right), \quad G_{\max} = 1000S_u \tag{3.4}$$

and

$$\frac{k_\theta}{k_{\theta,\max}} = 5.71\times10^{-5}\left(\theta^{-0.46}\right), \quad G_{\max} = 2500S_u. \tag{3.5}$$

These rotational stiffness degradation relationships for stiff clay correlate well with the test observations in Figure 3.7, although this approach needs further validation using data from more full-scale experiments with different parameters. Different types of clays, rotation amplitudes, footing sizes, and embedment configurations could be varied in these tests. A similarly broad study was performed for shallow footings on sand by Gajan et al. (2004), resulting in a recommended stiffness reduction trend of

$$\frac{k_\theta}{k_{\theta,\max}} = 3.0\times10^{-3}\left(\theta^{-0.6}\right). \tag{3.6}$$

## 4. CONCLUSIONS

Depending on the level of soil strain and loading type, rocking foundations may be able to dissipate large amounts of seismic energy through soil hysteresis as well as radiation damping caused by transient impacts. This understanding has led to recent research into the effectiveness of seismic energy dissipation by designing foundations to rock when subjected to dynamic loading. The results of a field investigation summarized herein generally support the claim that energy may be dissipated at the soil-structure interface. Rounding of the soil surface due to rocking-induced plastic deformations would require great care when identifying dynamic properties of these systems. Furthermore, the yielding soil would introduce nonlinearity into the response of the soil-foundation system directly influencing the period. A degradation of rotational stiffness was exhibited as soil was strained due to increasing amplitudes of rotation. Prior to developing rocking foundations for seismic loading, more field-scale experiments are recommended to study the effects of a variety of soil types, foundation sizes, and foundation shapes, and calibrate computational models such as the nonlinear contact interface model of Gajan and Kutter (2009).

## REFERENCES


Bartlett, P.E. (1976). Foundation rocking on a clay soil. ME Thesis. Report No. 154. University of Auckland, School of Engineering.

Gajan, S., Hutchinson, T.C., Kutter, B.L., Raychowdhury, P., Ugalde, J.A., Stewart, J.P. (2008). Numerical models for analysis and performance-based design of shallow foundations subjected to seismic loading. Pacific Earthquake Engineering Research Center. PEER Report 2007/04.

Gajan, S., Kutter, B.L. (2009). Contact interface model for shallow foundations subjected to combined cyclic loading. *Journal of Geotechnical and Geoenvironmental Engineering*. **135:3**, 407-419.

Gajan, S., Kutter, B.L., Phalen, J.D., Hutchinson, T.C., Martin, G.R. (2005). Centrifuge modeling of load-deformation behavior of rocking shallow foundations. *Soil Dynamics and Earthquake Engineering.* **25**,773-783.

Gajan, S., Phalen, J. D., Kutter, B. L., Hutchinson, T. C. and Martin, G. (2004). Centrifuge modeling of nonlinear cyclic load-deformation behavior of shallow foundations, *Proc. 11th Intl. Conf. Soil Dynamics and Earthquake Engineering* and *3rd Intl. Conf. Earthquake Geotechnical Engineering*. University of California, Berkeley. **Vol. 2**, 742-749

Gazetas, G. (1991). Chapter 15. Foundation engineering handbook. van Nostrand Reinhold, New York.

Seed, H.B., Idriss, I.M. (1970). Soil moduli and damping factors for dynamic response analyses. Report No.

EERC 70-10. Earthquake Engineering Research Center, UC Berkeley.
Shelman, A.T. (2009). Seismic design of drilled shafts in clay. MS Thesis. Iowa State University.